Energy Transformations in the East Asia–West Pacific Jet Stream

GEORGE P. CRESSMAN

National Meteorological Center, National Weather Service, NOAA, Washington, DC 20233

(Manuscript received 22 August 1983, in final form 19 December 1983)

ABSTRACT

Kinetic energy budgets were prepared for the East Asia–West Pacific region to obtain a quantitative description of the sources and sinks of kinetic energy for the jet stream of that region. Budgets were prepared for locations of jet stream acceleration and deceleration for the period 12–16 January 1979, during the Global Weather Experiment. The region of generation of kinetic energy in East Asia was characterized by a large-scale direct solenoidal circulation, with a five-day average generation rate of 95×10^{10} kW or 34 W m^{-2}. Orographic forcing over the east edge of the Himalayan plateau is suggested as a process partly responsible for the geographic reliability of the generation region over China. In the west Pacific region kinetic energy was destroyed by pressure forces at a rate of 61×10^{10} kW or 57 W m^{-2}. This region was characterized by a vigorous indirect solenoidal circulation. The kinetic energy generation and destruction took place mainly at jet stream levels and are seen as successive phases of a modified inertial oscillation of the jet. Kinetic energy conversion at these rates greatly exceeds that in a typical vigorous extratropical cyclone, which could be in the range of 10–20 $\times 10^{10}$ kW.

The subgrid-scale motions were a sink of kinetic energy during jet stream acceleration and a source during jet stream deceleration. This observation is confirmed on a more general basis by a literature review demonstrating a fundamental consistency among the many studies of the energetics of large-scale systems. The kinetic energy changes of the small (subgrid) scale flow paralleled those of the large-scale flow and were about 11 W m^{-2}. The magnitude of consistent subgrid- to grid-scale energy transfer over the Pacific (and elsewhere) indicates a need for considering the apparent phenomenon of negative viscosity in numerical atmospheric modeling.

1. Introduction

The acceleration of the air into the jet stream of East Asia and the West Pacific is the strongest that can be seen anywhere on wintertime climatological maps. The strength and steadiness of this circulation feature are portrayed in the atlas by Gray *et al.* (1976). This jet must result from the largest continuing kinetic energy production of the global atmosphere.

This production of kinetic energy takes place in a region of very large horizontal temperature contrasts. The continental arctic conditions over East Asia contrast with the heat and moisture available from the Bay of Bengal, the East and South China Seas and the West Pacific ocean. It is reasonable to expect that the available potential energy represented by these temperature contrasts is converted more or less *in situ* to fuel the accelerating jet stream.

The existence of a direct solenoidal circulation to accomplish this conversion has been known for many years. Staff members of the Academia Sinica (1957–1958) deduced mean vertical motions indicating a large-scale direct circulation. Mohri (1959) found evidence of a direct circulation around the wintertime jet stream over Japan. Murakami and Unninayar (1977), using operational analyses from the National Meteorological Center (NMC), outlined a large-scale direct circulation over East Asia for the 1970–71 winter. They showed the updraft part of the circulation over the Malaysia–Indonesia area and the sinking motion centered over north China. They pointed to the wet and cloudy weather over the Malaysia–Indonesia area as a major heat source to maintain the supply of available potential energy. Blackmon *et al.* (1977) concluded from a study of momentum flux that in the time-averaged flow there is a direct meridional circulation in the region of the jet stream acceleration. Vertical motions from short-range forecasts show a strong single-celled direct circulation centered on the East Asian–West Pacific upper front and jet stream, as shown by Cressman (1981).

Kung and Chan (1981) presented a kinetic energy budget computed directly from observations for a fixed area over eastern Siberia, eastern China, and the Sea of Japan for a two-year data period. Their winter budget showed a mean kinetic energy from the earth's surface to 10 kPa of 27×10^5 J m^{-2}. The mean generation was 14 W m^{-2}, with a net outward flux of 9 W m^{-2}, leaving about 5 W m^{-2} to be accounted for by dissipation. Although the location of their area was north of much of the jet stream, which is the zone of maximum kinetic energy, their study gives some confirmation of the earlier-mentioned studies and supplies some interesting quantitative results as well.

Farther east, over the central North Pacific, there is a wintertime area of diffluence in the middle and upper

troposphere flow and a persistent loss of kinetic energy associated with an indirect solenoidal circulation as discussed by Blackmon *et al.* (1977). Cressman (1981) presented additional data on this indirect circulation together with evidence that it is an inertial consequence of the direct circulation over East Asia and the West Pacific. This qualitative understanding can be put on a firmer basis by energy budgeting for the areas dominated by these two types of circulations. The objective of this study is to determine the rates and amounts of kinetic energy change in each type of circulation, what are the most important processes responsible and on what scale they act.

2. Preparation of the energy budgets

The jet stream over East Asia and the West Pacific is of variable vertical extent. Therefore the kinetic energy budgeting should include as much of the vertical extent of the atmosphere as possible. Volume integrals extending from the surface of the earth up to 7.5 kPa will be used.

The kinetic energy equation in the form used by Smith (1970) is convenient for energy budgeting of the atmosphere over a limited region σ of the earth's surface. It is

$$\partial K/\partial t = G(K) + B(K) + R. \tag{1}$$

The total kinetic energy K of the volume is

$$K = \frac{1}{g}\int_\sigma \int_{p_g}^0 \frac{\mathbf{V}\cdot\mathbf{V}}{2}\, dpd\sigma. \tag{2}$$

Its generation $G(K)$ is

$$G(K) = -\frac{1}{g}\int_\sigma \int_{p_g}^0 \mathbf{V}\cdot\nabla\phi dpd\sigma, \tag{3}$$

its increase due to boundary fluxes is

$$B(K) = -\frac{1}{g}\int_\sigma \int_{p_g}^0 \left[\nabla_p\left(\frac{\mathbf{V}\cdot\mathbf{V}}{2}\mathbf{V}\right) + \frac{\partial}{\partial p}\left(\omega\frac{\mathbf{V}\cdot\mathbf{V}}{2}\right)\right] dpd\sigma, \tag{4}$$

and the residual term is

$$R = \frac{1}{g}\int_\sigma \int_{p_g}^0 \mathbf{V}\cdot\mathbf{F} dpd\sigma. \tag{5}$$

The residual term R is sometimes referred to as a "dissipation." In practice it is obtained as a residual and includes a collection of measurement and computational errors. Positive values of R can mean subgrid- to grid-scale transfer of kinetic energy, the opposite of the ordinary meaning of dissipation. Therefore, in the following discussions R will be referred to as a "residual." The term "dissipation" will be reserved for energy exchanges in the direction from grid to subgrid scales.

The increase of gravitational potential energy due to vertical redistribution of mass within a region $I(P)$ is

$$I(P) = \frac{1}{g}\int_\sigma \int_{p_g}^0 \omega\alpha dpd\sigma. \tag{6}$$

The terms $G(K)$ and $I(P)$ are sometimes designated as conversion terms to be written as $C(A, K)$ and $-C(A, K)$ respectively, with $C(A, K)$ indicating conversion from available potential energy to kinetic energy. However, this is a correct interpretation only under a special and probably unattainable condition. As shown by Pfeffer (1957), ". . . the integrals which appear with opposite signs in the case of an *open* system have no significance as rates of conversion between two forms of energy unless the boundary integrals which couple the generation terms vanish identically."

Smith (1969) showed the linkage between the terms $G(K)$ and $I(P)$ in a form that will prove useful for this study. Using the gas law and the identity

$$\mathbf{V}\cdot\nabla\phi = \nabla\cdot\phi\mathbf{V} - \phi\nabla\cdot\mathbf{V}, \tag{7}$$

he integrated the continuity equation over the depth of the atmosphere and a limited area to obtain

$$\frac{1}{g}\int_\sigma \int_{p_g}^0 \omega\alpha dpd\sigma - \frac{1}{g}\int_\sigma \int_{p_g}^0 \mathbf{V}\cdot\nabla\phi dpd\sigma = -\frac{1}{g}\int_\sigma \int_{p_g}^0 \nabla\cdot\phi\mathbf{V} dpd\sigma - \frac{1}{g}\int_\sigma \int_{p_g}^0 \frac{\partial}{\partial p}(\omega\phi) dpd\sigma. \tag{8}$$

The symbols used are as follows:

- α specific volume of air
- g gravitational acceleration
- p pressure
- p_g pressure at the surface of the ground
- σ area of integration over the earth's surface
- ϕ geopotential
- ω dp/dt
- $\mathbf{F}$ frictional force
- $\mathbf{V}$ wind vector in a pressure surface.

The two right-hand terms of (8) represent the rate of work by the pressure forces on the boundaries of the volume. The two terms on the left of (8) are $I(P)$, from (6) and $G(K)$ from (3). The two integrals on the right side of (8) supply the linkage between $G(K)$ and $I(P)$.

The integral of $(\partial/\partial p)(\omega\phi)$ over the complete depth of the atmosphere is normally negligible. One might suppose that this integral could have some significance for a region containing the Himalayas but test evaluations showed all values to be less than 0.1 W m^{-2} for the areas used in this study. In future discussions this integral will be considered to have a value of zero.

Substitution into (8) from (3) and (6) and the application of Gauss's theorem to the third term of (8) yield for the limited volume

$$G(K) = -I(P) + \frac{1}{g}\oint_l \int_{p_g}^{0} \phi v_n dp dl. \qquad (9)$$

Here, dl is an incremental horizontal length around the periphery and v_n is the inward velocity component normal to the lateral boundary of the volume. This formulation presents the generation rate of kinetic energy inside the volume as a sum of the rate of decrease of potential energy by vertical displacements of air mass inside the volume and the geopotential fluxes into the volume. As pointed out by Palmén and Newton (1969), the last term of (9) can be thought of as giving the flux of potential energy into the volume. Examination of regions of kinetic energy generation can be made in terms of these processes.

The procedure to be used in the following sections will be to prepare kinetic energy budgets for three fixed atmospheric volumes. The first will be over the East Asia–West Pacific area where the wintertime jet stream shows a strong and nearly continuous acceleration. The second will be a subset of the first. The third volume will cover an area of the North Pacific where the wintertime jet stream undergoes nearly continuous deceleration. The areas of the earth's surface covered by these volumes will be referred to as areas A, B, C, respectively. Fig. 1 shows the speed of the five-day mean flow in the jet stream for the period to be studied and the locations of the three areas.

The calculations were needed for areas where the data supply is far from uniform. Over China there is a dense radiosonde network but over the Pacific the main data supply comes from surface ships, aircraft wind measurements, and satellite soundings. The calculations must be done consistently for all three volumes if meaningful comparisons are to be made.

The possibilities for initial data for the calculations were 1) the use of analyses from a high quality objective analysis system, 2) the use of analyses that have been initialized for a numerical forecast or 3) the use of information from a short-range numerical forecast. Of these three, the use of a 12 h forecast was selected. Uninitialized analyses are heavily influenced by a first guess from a previous forecast but their internal consistency leaves room for improvement, especially with regard to latent heating and its relation to divergence and the irrotational wind field. Currently available initializations are dry adiabatic and retain only the largest scales in the vertical motion field. Using a 12 h forecast as a data base subjects the energy analysis to the deficiencies of the forecast model used. However, the moisture field is brought into better agreement with the fields of the other elements during the first 12 h of the forecast, as shown by Lejenas (1979, 1980). This should help to improve the accuracy of the vertical motions and the irrotational flow in pressure surfaces. Therefore, as the best choice available, the 12 h forecast fields were used for all calculations to be presented.

The forecast model used was the spectral model of

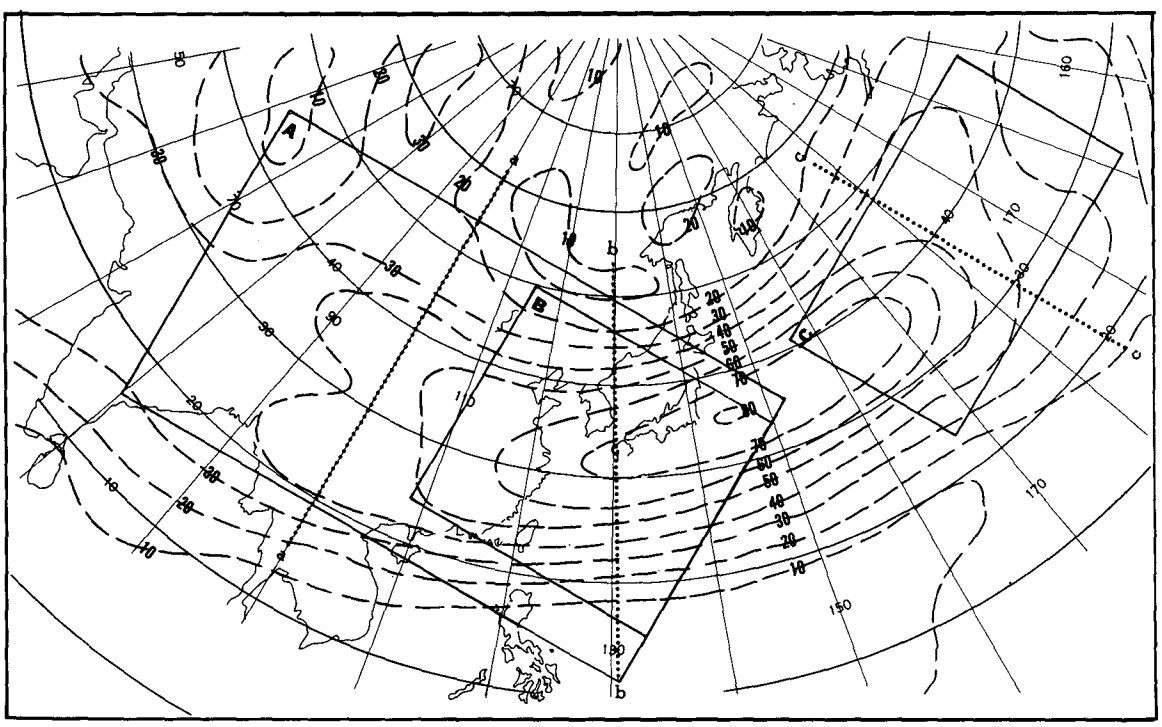

FIG. 1. Five-day mean isotachs (m s^{-1}) at 25 kPa for the period 1200 GMT 12 January 1979 to 1200 GMT 16 January 1979. The solid lines enclose areas A, B, C. Lines aa, bb and cc are the locations of the cross sections of Figs. 4, 5 and 6.

Sela (1980). Forecasts from this model have been widely available to the meteorological community for several years. Its level of performance is well known. In conformity with the arguments of Boer (1982) the numbers to be presented are averages of energy calculations made for individual days, in which no calculations were made for underground points. Results expressed in kilowatt units are 5-day averages of daily sums. However, results expressed in watts per square meter are the rates in watts divided by the total number of square meters in each area, both above and below the surface of the ground. This is done for consistency between the two sets of numbers and to avoid giving an exaggerated impression of the importance of energy exchanges over small fractions of each total volume.

The initial conditions for the forecasts were the IIIb analyses prepared for the Global Weather Experiment (GWE) period by the European Center for Medium Range Weather Forecasting. The initialization for the forecasts was by the nonlinear normal mode method (Machenhauer, 1977; Ballish, 1981). The forecasts were made at 24 h intervals from 0000 GMT data from 12–16 January 1979. This period was selected for analysis after an inspection of the 20 kPa isobaric analyses for January 1979 issued by the European Center for Medium Range Weather Forecasting. The period 12–16 January was characterized by an especially prominent acceleration in the SE Asian jet stream across China and into the Pacific Ocean. Average energy budgets for a longer period than the 5 days selected would be interesting in many respects. However, shifts in the jet location and strength that would be seen over a longer period might tend to smooth out the features to be examined, i.e., the strong acceleration and deceleration phases of the energy transformations in the jet.

The data for use in the energy calculations were taken from the 12 h forecasts at 5 kPa intervals on horizontal grids having a mesh length of 381 km at 60°N on a polar stereographic projection. In future discussions the term "subgrid scale" will be used to refer to scales of motion too small to be represented in a grid of this mesh length. The contribution of the atmosphere at pressures less than 7.5 kPa was neglected. Kinetic energy tendencies are computed as 96 h finite differences and other budget quantities are averages of those computed at 24 h intervals.

3. Results of the energy budget calculations

a. Asian area (A)

The kinetic energy budgets for all three areas for the five-day period are summarized in Table 1. Area A is quite large, covering 11% of the Northern Hemisphere. The average production of kinetic energy for the five-day period was 33.8 W m^{-2}, or 94.6 $\times$ 10^{10} kW. The net export (flux divergence) of kinetic energy averaged 22.4 W m^{-2} (62.7 $\times$ 10^{10} kW), showing that the export of kinetic energy was two-thirds of the generation rate. The net change of kinetic energy for the period was near zero, giving -11.4 W m^{-2} for the residual, which was 34% of the generation rate. This indicates grid to subgrid scale energy transfer.

Kung and Chan (1981) measured winter kinetic energy production over a large area of northeast Asia covering parts of Siberia, China and Japan, using observed winds and geopotentials. The average vertically integrated kinetic energy production was 13.7 W m^{-2}. For an area covering most of eastern China they found an average kinetic energy production of 60 W m^{-2}. Considering the differences in sizes and locations of the areas selected as well as the length of the periods studied the kinetic energy generation rate reported here is consistent with the rates reported by Kung and Chan.

Some idea of the significance of the rate of generation of kinetic energy for area A can be had by comparison with energy production rates in extratropical cyclones. Palmén and Newton (1969) stated that a "production rate . . . between 16 and 21 W/m^2 . . . may be considered characteristic of polar front cyclones in winter during their time of strong development."

More recently DiMego and Bosart (1982) presented a tabular review of 16 measurements of kinetic energy budgets of cyclones by various authors, published between 1971 and 1977. Twelve of these gave kinetic energy generation rates for extratropical cyclones. The average of these was 9.7 W m^{-2}. The five highest values shown were between 16 and 28 W m^{-2}.

Kung and Smith (1974) presented a kinetic energy budget for a typical large intense winter or spring cyclone, based on a review of the literature, giving a kinetic energy generation of 16 $\times$ 10^{10} kW. The area indicated was 10^{13} m^2, roughly one-third that of area A in this study. Comparison of the generation in area A with the typical rate given by Kung and Smith is revealing. It shows the kinetic energy generation for area A to be equivalent to the kinetic energy generation of six large intense winter cyclones on a continuous basis for the five days of the study period. In fact there were no surface cyclones within area A during these 5 days. A large anticyclone on the sea level map, starting at about 54°N, 96°E, moved southeastward, weakened and was replaced by another one at 48°N, 90°E by 16 January. The main surface flow in area A was in its east half and was a broad current flowing toward the southeast.

Figure 2a shows that the kinetic energy generation took place mainly at levels above the 50 kPa surface and was a maximum at the jet stream level, as shown by the $G(K)$ curve. The large values of the flux divergence of kinetic energy at the same levels show the large export of kinetic energy in the jet stream, which took place mainly through the east and northeast boundaries of area A. All nonzero values of the residual are negative (grid- to subgrid-scale energy transfer),

TABLE 1. Kinetic energy budgets for areas A, B and C for the period 12–16 December 1979. All numbers shown are volume integrals. Column headings are as follows:

K	mean kinetic energy
$G(K)$	generation of kinetic energy by pressure forces [Eq. (4)]
$B(K)$	flux convergence of kinetic energy [Eq. (5)]
$\Delta k/\Delta t$	rate of change of K for the 5-day period
R	residual [Eq. (1)]
$I(A)$	change of K by redistribution of mass by vertical motions [Eq. (9)]
$B(\phi)$	flux convergence of geopotential into the volume [last term of Eq. (9)]
$\bar{\omega}$	volume average of dp/dt for the period.

Area	K ($J\ m^{-2} \times 10^5$)	$G(K)$ (kW $\times 10^{10}$)	$G(K)$ ($W\ m^{-2}$)	$B(K)$ (kW $\times 10^{10}$)	$B(K)$ ($W\ m^{-2}$)	$\Delta k/\Delta t$ ($W\ m^{-2}$)	R ($W\ m^{-2}$)	$I(P)$ ($W\ m^{-2}$)	$B(\phi)$ ($W\ m^{-2}$)	ω ($Pa\ s^{-1} \times 10^{-2}$)
A—Asia $2.798 \times 10^{13}\ m^2$	32.9	94.6	33.8	−62.7	−22.4	0.0	−11.4	−302	336	1.6
B—Asian Coast $1.055 \times 10^{13}\ m^2$	52.6	49.2	46.6	−39.4	−37.3	−1.2	−11.5	−584	631	3.3
C—Pacific $1.086 \times 10^{13}\ m^2$	48.6	−61.3	−56.5	55.0	50.7	5.3	11.1	456	−513	−2.2

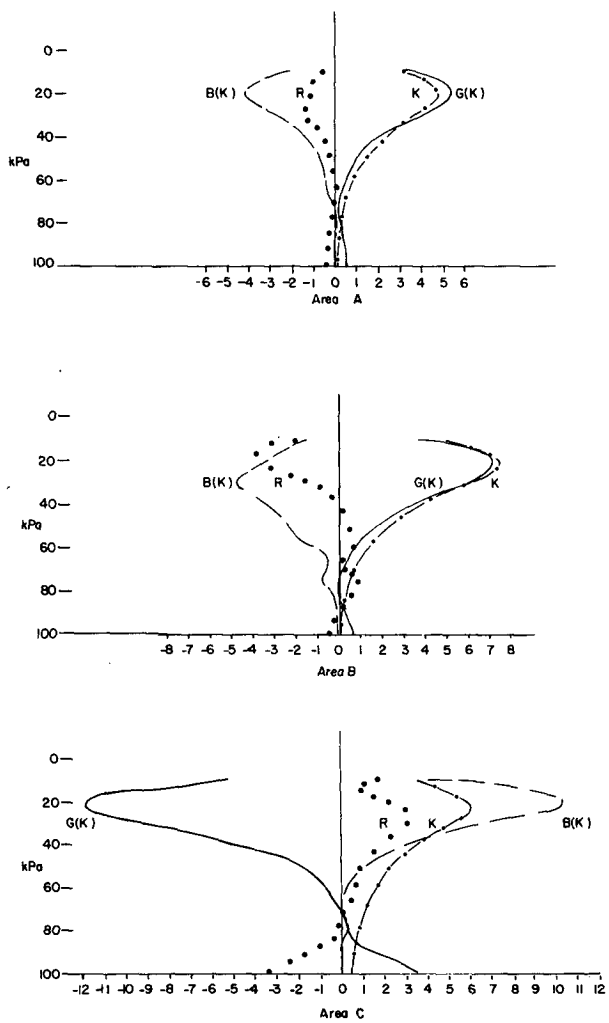

FIG. 2. Vertical distribution of the terms of the energy budget averaged for the five-day period for (a) area A, (b) area B, and (c) area C.

with a primary maximum at jet stream levels and a small secondary one below 85 kPa.

The average vertical motion in area A was downward, as shown from a volume average of ω of 1.6×10^{-2} Pa s^{-1} in Table 1. It gives a rate of decrease of gravitational potential energy, $-I(P)$, of 302 W m^{-2}. This contribution to loss of potential energy was more than balanced by flux convergence of geopotential $B(\phi)$ of 336 W m^{-2}. Since geopotential increases linearly with height a positive geopotential flux convergence indicates a high probability of a net inflow into the volume at high altitudes and, for mass continuity, a low altitude net outflow. This is not contradictory to the finding of a net flux divergence of kinetic energy. The flux divergence of kinetic energy is accomplished by the total wind, of which the rotational component is by far the major part. Geopotential flux divergence is accomplished by the ageostrophic wind component, which is only a small fraction of the total wind above the surface friction layer. At upper levels the ageostrophic wind component is also a good approximation to the irrotational wind component, outside of the equatorial region.

The high tropospheric net inflow can be seen from the 5-day mean 25 kPa velocity potential map shown in Fig. 3. The velocity potential maximum centered over China is the focus of the inflow. A large-scale irrotational inflow from the central Pacific, from area C of Fig. 1, is directed opposite to the total flow and toward China. The high tropospheric irrotational inflow from the south and west of China appears to come from rising air below the velocity potential minimum indicated by the dashed line of Fig. 3. East of 90°E this line marks an interruption of the large-scale upper-level irrotational flow from the equatorial zone toward the descent over China. The ascending branch of the circulation is over Indochina, the Bay of Bengal, India and the western Himalayas.

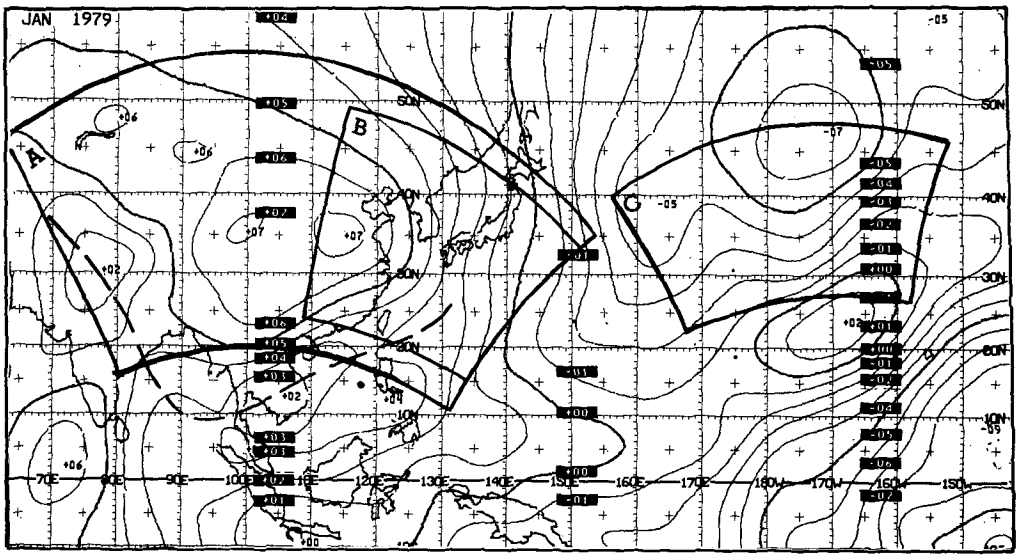

FIG. 3. Five-day mean velocity potential at 25 kPa for 1200 GMT 12 January 1979 to 1200 GMT 16 January 1979 in units of $m^2 s^{-1} \times 10^6$. Areas A, B and C in this projection are shown by the solid lines of medium weight.

The high-altitude inflow toward China, the average descent of the air in volume A listed in Table 1, and the rising motions near the south and west borders of Fig. 3 delineate a direct circulation cell over eastern Asia. The outer limits of this direct circulation (if they can be said to exist) must be outside the horizontal boundaries of volume A. Normally the wintertime northward high tropospheric irrotational flow into China originates farther south, as shown by Murakami and Unninayer (1977) as well as by regular monthly mean global velocity potential maps available from the National Meteorological Center. The 5-day period of 12–16 January 1979 seems to be anomalous in this respect.

Figure 4 is a 5-day mean cross section for the period 12–16 January 1979 along longitude 100°E, going through the broad velocity potential maximum of Fig. 3. It shows a large scale descent between 30° and 40°N, under the 25 kPa velocity potential maximum of Fig. 3. The strongest descending motions are located directly over the highest part of the terrain in the cross section. At this longitude the height of the ground begins its most rapid descent toward the east. This leads to the suggestion that the position of the maximum downward motion is centered over China during winter by orographic forcing as the upper westerlies descend after crossing the Himalayan plateau. This would be consistent with the center of kinetic energy generation being located over China during the winter, as indicated by the Kung and Chan (1981) regional energy measurements.

This suggestion is also in general agreement with that of Murakami (1981), who found evidence of an east–west circulation along the north side of the Asian plateau for the winter of 1978–79 and attributed it to mechanical forcing by the plateau.

b. Asian coast area (B)

This subset of the Asian area (A) was selected to allow examination of the region where kinetic energy production is likely to be the most active. Kung and Chan's (1981) calculations showing a maximum winter kinetic energy production over eastern China were used as guidance for selection of area B.

As shown by Table 1 the rate of generation of kinetic energy over area B, 46.6 W m^{-2}, was 1.4 times that of area A. The total generation, 49.2×10^{10} kW, was smaller because of the smaller size of area B. The flux divergence of kinetic energy from area B was 37.3 W m^{-2}, 80% of the generation rate. The residual, −11.5 W m^{-2} again indicates grid to subgrid scale transfer of kinetic energy at 25% of the generation rate.

The generation of kinetic energy for area B for the 5-day period was three times that of the typical large cyclone of Kung and Smith (1974) for an area almost the same size as that of their cyclone. By comparison with the kinetic energy generation (and export) over areas A and B it is evident that extratropical cyclones should not necessarily be considered as the major source of kinetic energy in the winter atmosphere. The production of kinetic energy over the nearly steady low level cold flows from continents toward tropical oceans may well be of greater importance.

Figure 2b shows that the generation and flux divergence of kinetic energy took place almost entirely at pressures less than 70 kPa and were a maximum

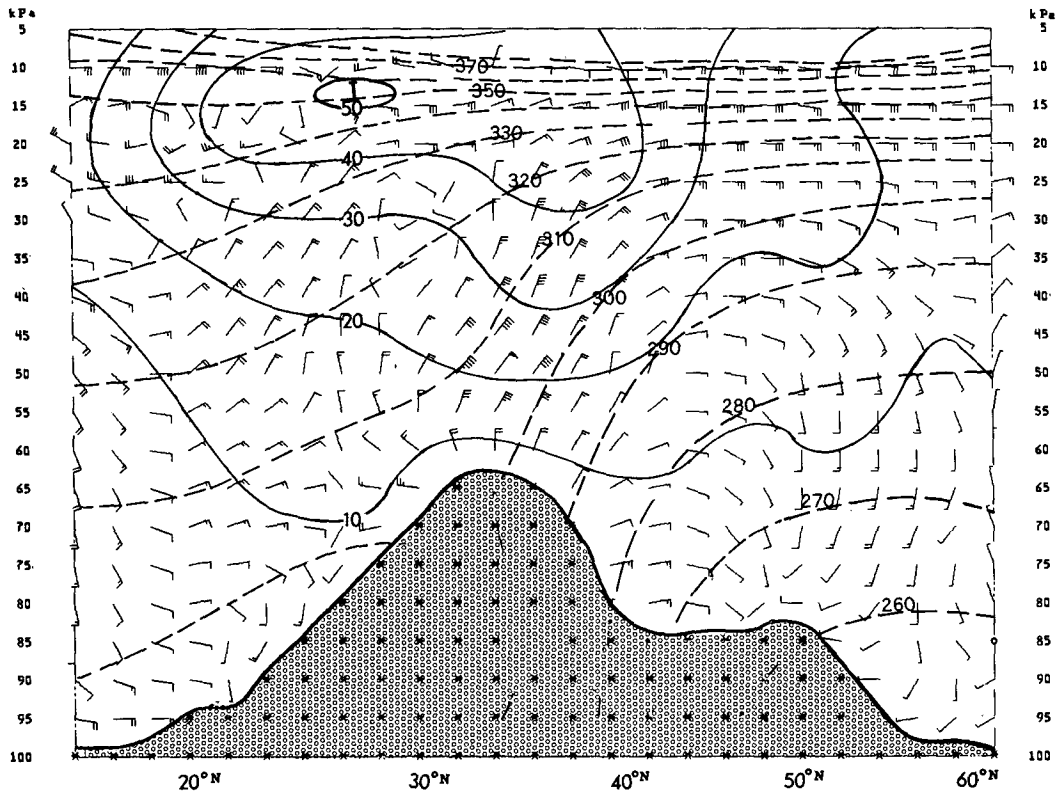

FIG. 4. Five-day mean cross section along 100°E for the period 1200 GMT 12 January 1979 to 1200 GMT 16 January 1979. Solid lines are isotachs of wind speed (m s^{-1}) and dashed lines show potential temperature. The vectors show the divergent component of the flow projected into the plane of the cross section. Their horizontal components represent the irrotational flow in the isobaric surfaces. Their vertical components represent the individual pressure change dp/dt. The two components are scaled by an approximate vertical to horizontal scale ratio in the atmosphere of 100 kPa/$10^6\sqrt{10}$ m. The vectors are plotted as in standard synoptic practice, e.g., a full barb is 10, etc. A horizontal vector of value 10 represents 1 m s^{-1} and a vertical vector of value 10 represents $dp/dt = 3.16 \times 10^{-2}$ Pa s^{-1} or 2.73 kPa day^{-1}. The smoothed height of the terrain in the plane of the cross section is indicated by a solid line.

at jet stream levels, as was the case for the entire area A.

The mean sinking motion for area B, 3.3×10^{-2} Pa s^{-1} was twice that for area A. The rate of loss of potential energy by this sinking motion was 584 W m^{-2}. Flux convergence of geopotential into the volume was 631 W m^{-2}, indicative of a pronounced high level net inflow into the area. Continuity of mass requires a compensating low level net outflow.

Figure 5 is a 5-day mean cross section along 130°E, through area B. It shows a direct solenoidal circulation with descending motion on the cold side of the jet and ascending motion on the warm side. The jet stream is better developed in this cross section than in the one of Fig. 4 for 100°E as a consequence of the strong kinetic energy generation taking place between these longitudes.

c. *Pacific area* (C)

The approximate location of the area selected for budgeting over the North Pacific was determined on the basis of an earlier study linking positive and negative regions of kinetic energy generations in the jet stream to the dimensions of a modified inertial cycle (Cressman, 1981). Its exact position was determined after inspections of maps of $-\mathbf{V}\cdot\nabla\phi$ at 25 kPa for each of the days. The area is 4.3% of the Northern Hemisphere, about the same as that of area B. Area C yields almost the reverse of area B for kinetic energy budgeting. The average $G(K)$ is -56.5 W m^{-2} or -61.3×10^{10} kW. The flux convergence of kinetic energy was 50.7 W m^{-2}. During the period from 12 to 16 January the kinetic energy in the volume increased from 37.9×10^5 to 56.2×10^5 J m^{-2}. This gives a residual of 11.1 W m^{-2} for the period, which is 20% of the magnitude of the generation rate. Here the residual acts as an energy source for the grid-scale energetics.

Since the 5-day average vertical motion in area C was upward, at a volume-averaged value of -2.2×10^{-2} Pa s^{-1}, the gravitational potential energy was increasing at a rate of 456 W m^{-2}. This was more than compensated by a rate of geopotential flux divergence

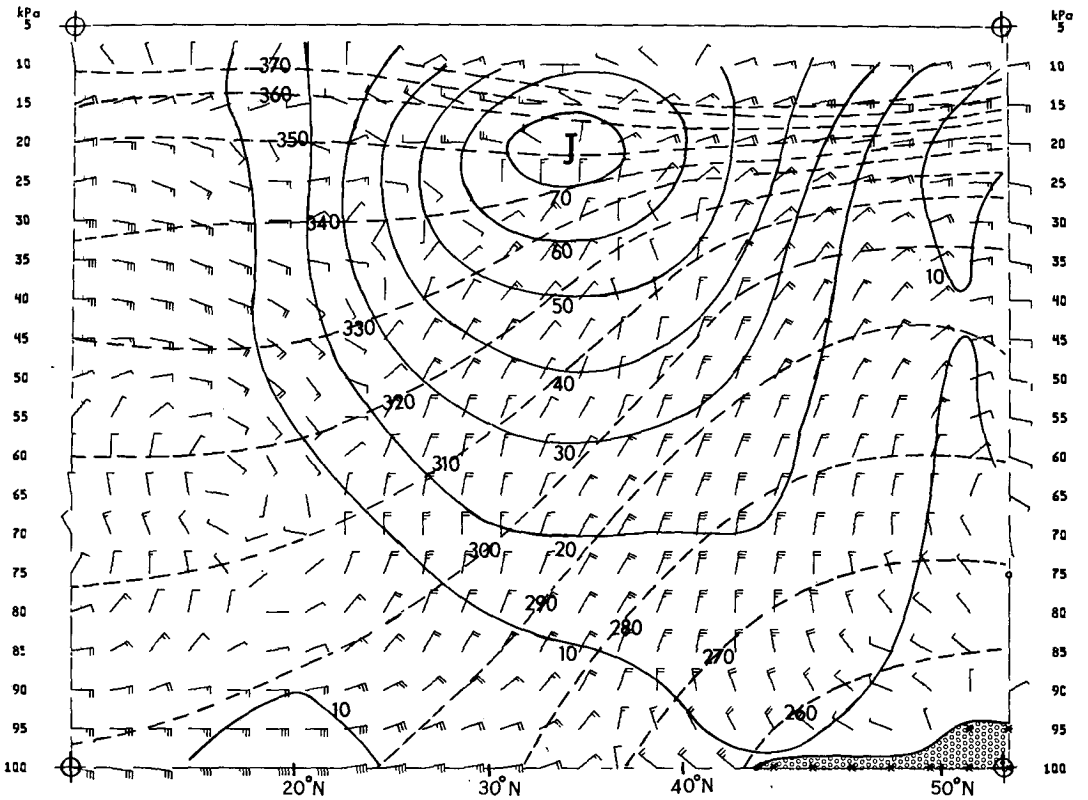

FIG. 5. Five-day mean cross section along 130°E. Details as in Fig. 4.

of 513 W m^{-2}, indicating a large-scale net outflow at upper levels. As shown by Fig. 3 the outflow of the irrotational circulation was most pronounced toward the south and toward the west. Of course, on charts of the total flow the outflow of the irrotational circulation is masked by the strong rotational flow and is impossible to see. The focus of the outflow to the south for this 5-day period is the velocity potential maximum at 24°N, 168°W, within the winter rainfall minimum of the central Pacific.

The distribution of the energy budget components in the vertical is shown in Fig. 2c. The maximum destruction of kinetic energy by the pressure forces, $-G(K)$, is shown at the jet stream level, as is the maximum of flux convergence of kinetic energy. At levels below 70 kPa there was a generation of kinetic energy. This is not surprising, since a very active frontal system occupied area C for the five-day period, during which an occlusion, three developing wave cyclones and a strong cold air pressure trough moved through the area. All these developments notwithstanding, the energy destruction at middle and upper atmospheric levels completely dominated the energy budget. The dominance of the active frontal systems in kinetic energy production was limited to levels below 70 kPa.

Figure 6 is a 5-day mean cross section extending approximately from south to north through the middle of area C. A vigorous indirect solenoidal circulation dominates the cross sections. The convergence of irrotational flow at high levels between 20° and 25°N in the cross section agrees well with the velocity potential maximum shown in Fig. 3. The strongest descent is found in the warm air under this upper convergence region. The strongest ascending motion is shown between 45° and 50°N, well within the cold air.

4. Kinetic energy dissipation in the jet stream region

The residuals are obtained as relatively small differences between terms four times larger. It is natural to be concerned about the accuracy of the values obtained. This is especially true if the residuals are positive, indicating the subgrid-scale motions to be a source of kinetic energy. This invokes the idea of negative viscosity (Starr, 1968). It creates difficulties because the subgrid-scale motions are as yet indescribable and their interaction with grid-scale motions even more so. However, positive residuals as defined in (1) and (5) appear with some frequency in the literature on kinetic energy budgets.

In many studies of kinetic energy budgeting the significance of the results is estimated by randomly perturbing the data with errors of a reasonable size and